Adsorption 6, 93–104 (2000)

Transient Thermal Study of an Adsorption Refrigerating Machine

L. LUO AND D. TONDEUR
Laboratoire des Sciences du Génie Chimique-CNRS-ENSIC-INPL 1, rue Grandville, B.P. 451, 54001 Nancy, France

Received August 18, 1997; Revised April 15, 1999; Accepted April 28, 1999

Abstract. Adsorption refrigerators are a particular type of refrigerator in which compression is avoided, and in a sense replaced by adsorption. No mobile parts are needed; the energy input, instead of being mechanical, is thermal and is used to achieve desorption. Such machines have a cyclic operation, made of successive adsorption/evaporation and of desorption/condensation steps.

The transient operation of adsorption refrigerators is a relatively recent subject of research. The modeling of the adsorber is the key point of such studies, because of the complex coupled heat and mass transfer phenomena that occur during the cycle. The present work therefore presents a study of an annular type adsorber which is intended to account for transient temperatures observed experimentally. The equipment in which the experiments were performed and which uses alcohol adsorption on activated carbon is briefly described, and its operating cycle described, along with typical experimental observations of pressure and temperature transients. A model of the adsorber unit is proposed which accounts for the coupling of adsorption and heat transfer, and describes mass-transfer in the annular adsorbent layer as a global diffusional mechanism with temperature dependent parameters. This model correctly predicts, qualitatively and semi-quantitatively, the observed trends of the temperature changes. Finally, various aspects of the performances are discussed.

Keywords: adsorption refrigerator, transient operation, activated carbon, methanol, modeling

I. Introduction

The present concern about global environment and the protection of the ozone layer questions the nature of the cryogenic fluids used in common compression refrigerators, and encourages the development of different types of thermal machines. Most such machines presently commercial are based on liquid-vapour absorption.

Refrigerating machines based on vapour-solid adsorption are an interesting alternative because of the reversibility of adsorption mechanisms, and of their relatively simple technology and operation. In spite of the existence of a number of applications, these machines remain complex with respect to their scientific study, both theoretically and experimentally.

Many researches done on this type of machine are global studies (Luo et al., 1994; Critoph and Vogel, 1986), aiming at global average performances. However, since the operation of these machines is transient, and involves discrete steps, implying the optimal choice of step duration, a good knowledge of the transient regimes is essential.

Detailed and global models for cyclic absorption are numerous, and can be found in books like that of Ruthven (1984), Yang (1987) and Suzuki (1990). More specific models for sorption refrigerators have been developed for example by Sakoda and Suzuki (1984), Sun and Meunier (1987), Spinner et al. (Lu et al., 1996).

Although a model is presented in the present work, which accounts in some detail for the thermal and physical properties of the system, the focus is not on

improving models, but rather on observing, explaining and predicting the transient behaviour of the characteristic variables in such a machine, inasmuch as they are determined by the adsorption/desorption process.

In a first part of the present paper, we describe the experimental prototype and its operating mode compared to a theoretical cycle. In the second part, we introduce the model, and compare simulation results with some measured results. Finally various aspects of modeling, of performances and of optimization are discussed.

Let us emphasize that the overall time-scale of the cycle chosen here is roughly that of a night/day type of cycle, in which the heating of the adsorber would be effected using solar energy for example.

II. Description and Operation of the Adsorption Refrigerator

Figure 1 illustrates the flowsheet of a quadri-thermal adsorption-refrigerator, comprising a condenser, a throttle valve and some conventional valves, an evaporator, an adsorber and a circulating fluid (here, methanol).

In the experimental prototype, the condenser is a bottle of volume 0.52 liters, cooled by a water circulation coil. The evaporator is a finned-tube heat exchanger, placed in a cooling box. The adsorber is the essential element in this design (Fig. 2). It is a cylindrical tube (length 1.06 m, inner diameter 0.06 m, wall thickness 0.002 m) with an inner stainless steel cylindrical grid (length 0.95 m, diameter 0.02 m) allowing the adsorbent to be held in the annular space. This inner cylinder is connected at one end to the external fluid circuit. The adsorber can be heated by an electric wire wrapped around it, allowing a maximal surface heat

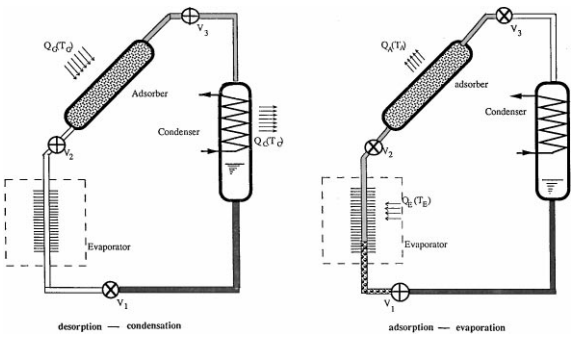

Figure 1. Flowsheet of an adsorption refrigerator showing the two half-cycles.

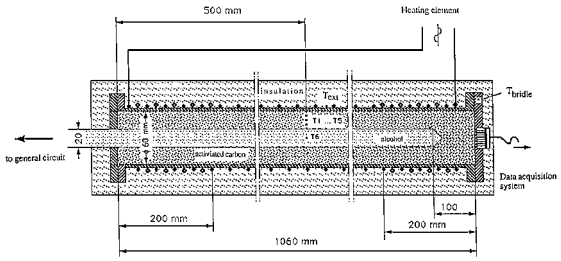

Figure 2. Construction of the annular adsorber.

flux of 750 W/m^2, and the whole system is properly insulated A vacuum pump is included in the circuit, achieving a vacuum of 3 Pa for a good initial desorption of the adsorbent. The vacuum pump is not used in normal cyclic operation.

Measurement devices include 11 thermocouples, (8 of which are located in the adsorber, as shown on Fig. 2), three pressure sensors, a fluxmeter located at mid-length on the external surface of the insulation, and a liquid level measurement in the condenser. Data acquisition is made on a personal computer. The fluxmeter will serve in determining an overall heat transfer coefficient between the insulated adsorber and the outer atmosphere. The adsorbent is activated carbon AC 35/3 of CECA (extruded cylinders of 0.0035 m diameter). The mass of adsorbent is 0.86 kg. The adsorbing fluid is methanol. During the adsorption-evaporation half-cycle, the methanol vapour flows from the evaporator to the inner cylinder, where it "diffuses" into the carbon layer.

In this section, we shall simultaneously describe the physical operation of the apparatus, the thermodynamic cycle, and the time-evolution of some key measured variables during a typical cycle. This paralled approach provides, we believe, a better understanding of the observed behaviour, of the underlying physical phenomena, and of the scientific and technical questions at stake.

Adsorption Versus Compression Refrigerator

Let us first observe that, compared with a conventional compressor-refrigerator, working basically according to an inverse Carnot-cycle, the fundamental difference is that the compressor is in a sense replaced by the adsorber. This has a series of important implications.

— the circulating fluid undergoes not only conventional P, V, T changes and evaporation-condensation

but in addition adsorption-desorption; its thermodynamic cycle can therefore not be represented conveniently on a (P, V) or a (T, S) diagram;
— fixed-bed adsorbers necessarily operate discontinously and therefore the operation of the adsorption-refrigerator is also discontinuous (cyclic);
— the auxiliary driving energy is not mechanical or electrical to drive the compressor, but thermal, and stems from the necessity to heat the adsorbent; low level heat or solar energy may be used for that purpose.

This heating step plays the role of the compression, and indeed corresponds also to a pressure increase.

Theoretical Cycle

A typical theoretical cycle comprises four distinct steps, which are:

1. a throttling-evaporation-adsorption step, in which the useful cooling effect is obtained;
2. an "isosteric" heating step of the adsorber, as discussed above;
3. a desorption-condensation step
4. an isosteric cooling step of the adsorber.

Such a cycle, in its "ideal" version, can be most conveniently represented schematically on a (P, T) diagram, combined with a plot of adsorbate content q of the adsorber (Fig. 3). The quantities plotted here are relative to the inside of the adsorber. The numbering of the steps corresponds to their definition given above.

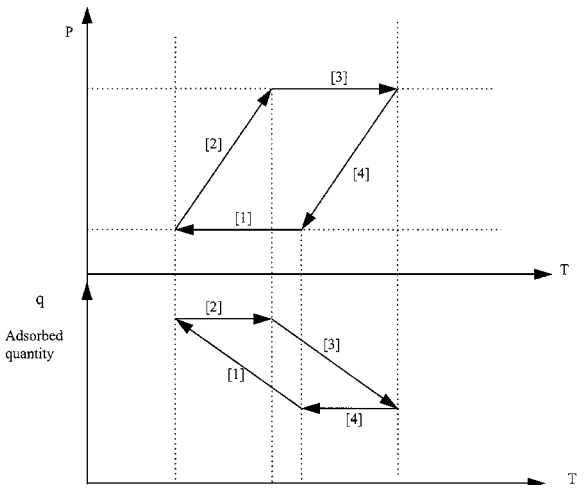

Figure 3. Ideal cycle on pressure-temperature and adsorbed quantity-temperature diagram.

Let us comment on this schematic cycle. In step 1, cold alcohol flows from the evaporator to the adsorber, where it is adsorbed. Simultaneous removal of the heat of adsorption is effected, using external cooling; the pressure is essentially constant.

In step 2, the adsorber is isolated and heated by external means; thus pressure and temperature rise simultaneously, while the global adsorbate content of the adsorber remains constant. In step 3, the adsorber being connected to the condenser, desorption occurs (q decreases) while the external heating continues (T increases, P is essentially constant). In step 4, the adsorber is isolated again (q is constant) while it is being cooled externally (T and P decrease).

Let us insist on the fact that this is a schematic representation of a theoretical cycle. As we shall see on the experimental results, the actual evolutions are more complex. It is one of the purposes of the present article to explain and discuss the actual transient behaviour.

Actual Operation of the Apparatus

Figure 4 is an experimental illustration of pressure and temperature changes actually measured in the adsorber during a complete cycle.

Step 1. We start with the adsorption-evaporation step by opening the throttling valve V1, and the ordinary valve V2, while V3 is closed. The liquid methanol is throttled through V1 from the condenser to the evaporator, where it is vaporised and produces a useful cooling effect. The vapour flows further through V2 to the adsorber, which acts as a sink for matter.

There is first a quasi-instantaneous pressure due to pressure equilibration between the adsorber (initially at about 7 mbar) and the evaporator (at about 25 mbar). Adsorption occurs immediately, with rapid heat release, and a sharp temperature rise is also observed. We first notice that both these pressure and temperature transients are not accounted for in the theoretical cycle of Fig. 3, where the heat released by adsorption is ignored, or assumed to be removed instantaneously by cooling. After this initial short transient, slower changes set in: a decreasing flow of methanol continues toward the adsorber, while the heat of adsorption is more than compensated by external cooling (natural cooling in our experiment) and by the sensible heat of the cold methanol. The temperature thus decreases

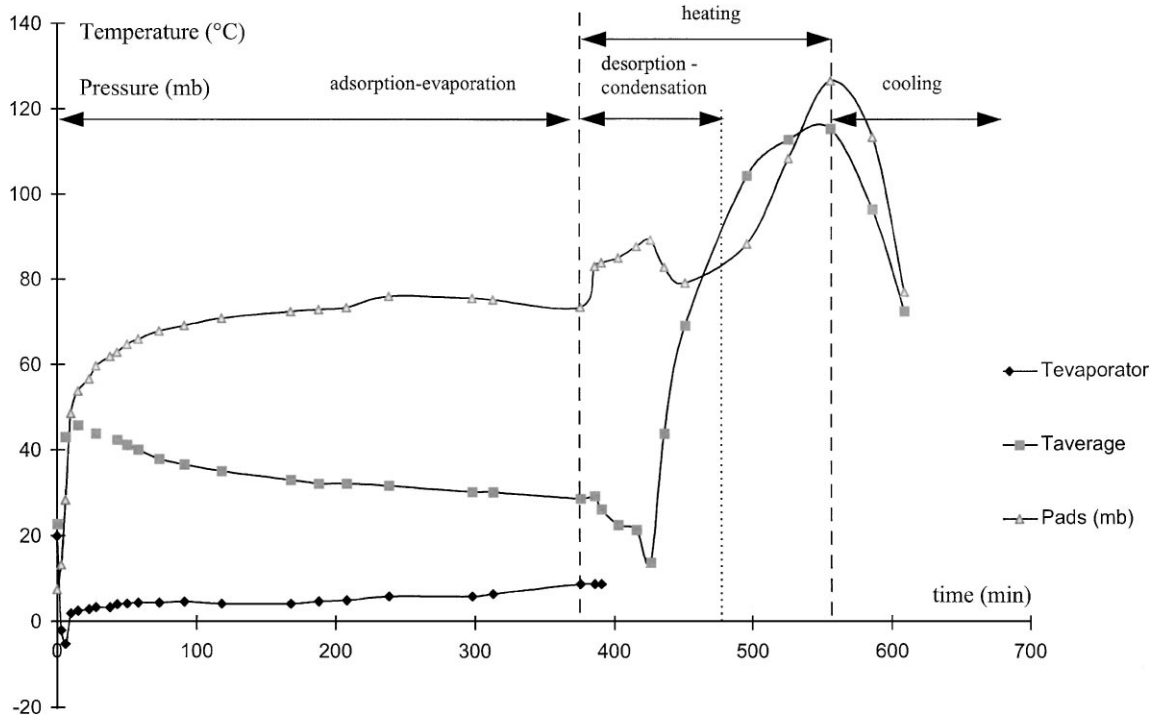

Figure 4. Temperature and pressure evolution for a complete cycle measured in the adsorber.

slowly, while the pressure remains practically constant. This slow evolution is qualitatively consistent with traject 1 in Fig. 3.

Steps 2 and 3. In the procedure followed here, there is no isosteric heating step, and the adsorber is not isolated. Thus steps 2 and 3 are combined. This is achieved by closing valves V1 and V2, opening V3, starting circulation of cooling water in the condenser, and starting heating the adsorber. These simultaneous events result in rather complex transients, of which only an overall result is observed on Fig. 4.

Opening valve V3 results in a pressure equilibration between the adsorber (here initially at about 75 mbar) and the condenser which is at a somewhat higher pressure (220 mbar). This may produce some instantaneous backflow of methanol from the condenser to the adsorber and readsorption, with a corresponding temperature increase, hardly seen in the present example. When condensation sets in, this flow is immediately reversed and results in rapid desorption, and a corresponding decrease in temperature due to the heat of desorption. After these initial transients, the external heat brought to the adsorber overcompensates the heat of desorption, and the temperature rises, producing further desorption. The pressure first decreases than increases with temperature during this period.

Step 4. When the condensing flow becomes very small, valve V3 is closed, the heating of the adsorber is interrupted, and the isolated adsorber is let to cool with a constant content of alcohol. Both pressure and temperature decrease.

It can be seen that the evolution of the variables is much more intricated than in the theoretical cycle. This is due essentially to the combination of three factors:

— the instantaneous effects of pressure equilibrations when valves are opened
— the fast effects of heat of adsorption, or desorption.
— the slow heat exchange of the adsorber with its surroundings, resulting in delayed effects of setting in this exchange.

In addition to these physical processes, two important design or operation factors influence these cycles: the scheduling of the cycle, and the amount of methanol present in the system. The transient behaviour illustrated above is not the only one possible, and different

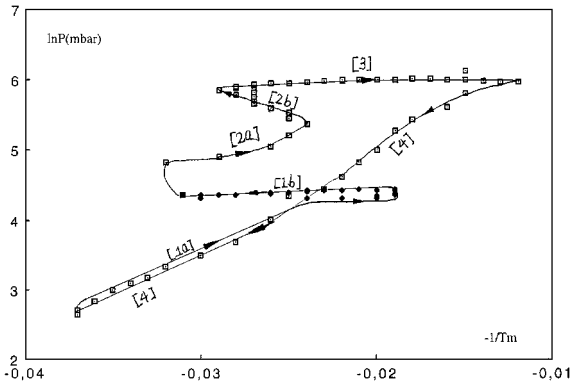

Figure 5. Clapeyron diagram of P and T measured in the adsorber for a typical cycle.

patterns may appear when one looks at details on a finer time scale, although of course the general evolution is conserved. For example, Fig. 5 represents a typical complete night/day type of cycle on a Clapeyron diagram, qualitatively analogous to the (P, T) diagram of Fig. 3. The cycle described here is the fourth after a start-up, and the behaviour of subsequent cycles is essentially periodic.

Adsorption with rapid heat release corresponds to path [1a], and the slow fall of temperature at constant pressure is presented by line [1b]. During the desorption, the temperature increases (line [2a]) then decreases (line [2b]) corresponding to the readsorption and desorption as mentioned in relation to Fig. 4. After these initial transients, the temperature rises due essentially to external heating (path [3]). Contrarily to Fig. 4, the pressure is practically constant during these steps. Path 4 corresponds to the cooling period.

III. Modeling the Adsorber

The model presented below concerns the slow adsorption and desorption steps of the cycle. The fast pressure transients due to valve manipulation are not modelled here. Neither is the "natural" cooling step (step 4). The model below thus applies to steps 1 and 3 of the theoretical cycle.

The assumptions underlying this model are listed below:

H1: During each step 1 and 3, the pressure is assumed constant (but different in the two steps)
H2: Thermal equilibrium is achieved locally between the solid and the fluid in the adsorber
H3: The temperature and concentration in the adsorber are assumed axially homogeneous (but dependent on radial position).
H4: The gas phase is assumed perfect.
H5: Adsorption equilibrium is assumed locally between fluid and adsorbent (no mass-transfer resistance at the fluid/solid interface).
H6: Radial heat and mass transfer are described by an equivalent diffusional mechanism (natural and forced convection are neglected).

The justification of assumption 1 is illustrated by the two horizontal parts on Fig. 5, both corresponding to a long time period. This is typical of the steady cyclic regime we observed, although sometimes, some pressure changes were observed, analogous to that of Fig. 4. Aside from these transients, mainly related to valve switching, as discussed above, it is seen that the pressure tends to be "stable" around two values, one typical of the adsorption step (around 75 mbars here), and one typical of the desorption step (around 400 mbars here). The maximal deviation from this average being about 15%, it is not unreasonable to assume constant pressure. Assumption H3 was justified by separate measurements of the axial temperature profiles at a middle radial position, which showed homogeneity except for some end effects.

With these assumptions, a local material balance on a differential annular element of adsorbent (Fig. 6) can

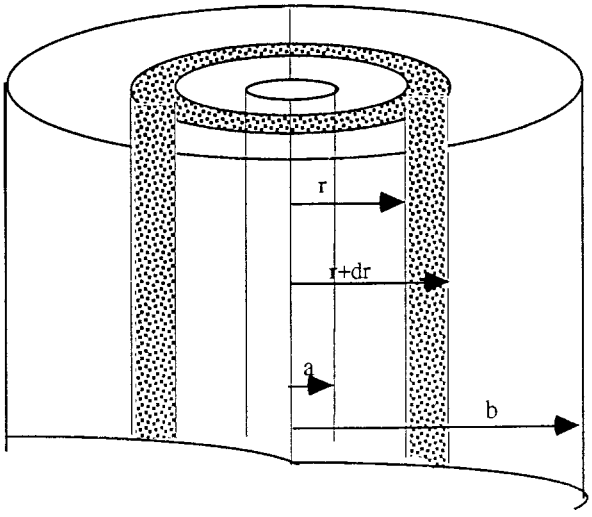

Figure 6. Geometric variables in annular adsorber.

be written as:

$$\varepsilon\frac{\partial C}{\partial t}+(1-\varepsilon)\rho_s\frac{\partial q}{\partial t}=\frac{\varepsilon}{r}\frac{\partial}{\partial r}\left[Dr\frac{\partial C}{\partial r}\right] \qquad (1)$$

The left-hand side represents the accumulation of methanol in the porous space and as adsorbed phase; the right-hand side represents the net diffusional flux into the annular element. Recalling that the only gaseous species present in the system is methanol, it appears that D is not a true diffusion coefficient, but rather a permeability. The driving force for penetration of methanol into the layer of activated carbon particles is a pressure gradient, proportional to the concentration gradient. In the calculations, D was estimated by a modified correlation for bidisperse systems inspired by Boussehain (1986) and given in Appendix. The initial and boundary conditions for Eq. (1) are of the following type:

$$\begin{aligned}&\text{I.C.}\quad t=0,\quad a<r<b,\quad C=C_i\\ &\qquad\text{(initial concentration profile of the step)}\\ &\text{B.C.}\quad t>0,\quad r=b\quad \frac{\partial C}{\partial r}=0\\ &\qquad t>0,\quad r=a\quad C=C_f\end{aligned} \qquad (2)$$

for adsorption, C_f is the concentration of the vapour from the evaporator; for desorption, C_f is taken to correspond to the vapour pressure at the condenser conditions.

The energy balance is expressed in the following way:

$$\frac{\partial T}{\partial t}[\varepsilon C C_{vg}+(1-\varepsilon)\rho_s(C_{vs}+qC_{va})]+(1-\varepsilon)\rho_s\Delta u_{ad}\frac{\partial q}{\partial t}=\frac{1}{r}\frac{\partial}{\partial r}\left[\lambda_{eff}\frac{\partial T}{\partial r}\right] \qquad (3)$$

To obtain this form, we have neglected the net enthalpy transported by the diffusion flux and the term $\frac{\partial P}{\partial t}$ because of assumption H1. λ_{eff} is an effective thermal conductivity and Δu_{ad} is the molar energy of adsorption. The boundary and initial conditions are:

$$\text{B.C.}\quad t>0,\quad r=a,$$

$$-\lambda_{eff}\left(\frac{\partial T}{\partial r}\right)_{r=a}=K_i(T_{r=a}-T_e)\quad\text{for adsorption} \qquad (4a)$$

$$=0\quad\text{for desorption} \qquad (4b)$$

$$t>0,\quad r=b,$$

$$-\lambda_{eff}\left(\frac{\partial T}{\partial r}\right)_{r=b}=K_0(T_{r=b}-T_o)+P_u \qquad (4c)$$

P_u represents the external heating power, assumed constant in the present approach; $P_u=0$ for adsorption, $P_u\neq 0$ for desorption;

$$\begin{aligned}&\text{I.C.}\quad t=0\quad T=T_{ia}\quad\text{for adsorption}\\ &\qquad\qquad T=T_{id}\quad\text{for desorption}\end{aligned} \qquad (5)$$

The boundary conditions (4a and 4c) express an overall conductive heat transfer mechanism at the boundaries of the carbon layer. During desorption, there is no axial flow in the center tubing, and thermal equilibrium is assumed between the inner carbon layer boundary and the center tubing.

The material balance (1) and the energy balance (3) are coupled through the dependence of q on C or T, and the dependence of the physical parameters (ΔU_{ad}, C_{vg}, C_{vs}, λ_{eff}, D) on both temperature and concentration. These variations are all accounted for in the calculation, using the relations given in Appendix.

The adsorption isotherm used is that of Dubinin-Raduschkevitch (Luo, 1991)

$$\frac{q}{q_m}=\exp\left[-k\left(\frac{\varepsilon'}{\beta}\right)^2\right] \qquad (6)$$

where q_m is the maximal adsorbed amount, estimated from the pore volume of the particles and the molar volume of liquid methanol. The Polanyi adsorption potential ε' is given by:

$$\varepsilon'=-RT\ln\frac{P}{P_{sat}}=-RT\ln\frac{RTC}{P_{sat}} \qquad (7)$$

where P_{sat} is the saturation pressure at T.

The set of constitutive Eqs. (1) and (3), (with the initial and boundary conditions (2, 4, 5) and the complementary Eqs. (6) and (7), are solved using an explicit finite difference scheme for the time variable, with a convergence test, and a centered difference for space. From the numerical values obtained for C and q, some overall material quantities may be calculated such as:

— the flux of matter entering or leaving the module (m_e for adsorption, m_0 for desorption), equal to the flux diffusing through the internal cylindrical boundary:

$$m=2\pi aL\left(D\frac{\partial C}{\partial r}\right)_{r=a}$$

— the total amount of methanol processed

$$m_{tot}=\int_o^t m\,dt$$

— the total adsorbed quantity

$$Q_{\text{tot}} = \int_a^b 2\pi r L \rho_s q \, dr$$

Comparison with Experimental Results

A number of cyclic experiments have been run, during which the transient values of temperatures, pressure, and quantities of methanol processed have been measured. The influence of various operating parameters has also been examined.

The lowest temperature recorded on the surface of the evaporator tube was $-10°$C, during the first cycle. In cyclic steady state, this temperature stays around $0°$C.

The following results concern essentially the temperature measurements inside the adsorber. Figure 7 shows an example of temperature evolution during the evaporation-adsorption step, at different radial positions, with both calculated curved and some measured points. It is seen that the overall trends are in reasonable agreement. However, the calculated curves inside the adsorber are below the measured curve, which suggests that we probably underestimated the mass flux parameter, that is, the effective diffusion coefficient. Note that the latter is obtained as a function of temperature by the semi-empirical formula of Boussehain (Boussehain, 1986) given in Appendix. No fitting of parameter is done here.

The general shape of the curves and the fact that two temperature curves (for $r = 10$ mm and $r = 20$ mm) cross each other, are explained as follows. At the beginning of the adsorption step, adsorption takes place essentially at the inlet of the adsorbent layer ($r = 10$ mm), where there is little resistance to mass transfer, resulting in a rapid adsorption accompanied by a rapid temperature increase. Inside the adsorbent layer ($r = 20$ mm), the rate of adsorption, and therefore the rate of heat release, is limited by penetration of adsorbate into the layer, resulting in a slower temperature rise and a lower initial temperature peak. For larger times, the inlet part of the adsorbent becomes saturated with adsorbate, and is progressively cooled by cold gas coming from the evaporator. This cooling effect is of course slower inside the layer and therefore the temperature at $r = 10$ mm can become smaller than that at $r = 20$ mm. Near the outside wall ($r = 30$ mm), thermal losses to the outside are responsible of the lower position of this curve.

Figure 8 shows the same comparison for the desorption step. Again, the model predicts the trends, which can be explained as follows:

— the desorption is produced by heating externally the adsorber and by opening the connection with the condenser. Initially, the adsorber is at a pressure lower than the condenser. When valve V3 is opened, there is some backflow from the condenser to the adsorber, producing possibly some readsorption. As the temperature rises in the adsorber, so does the pressure, and flow of alcohol from adsorber to condenser takes place. At the beginning of this step, the temperature increase is due to the external heating but possibly also to some readsorption, and of

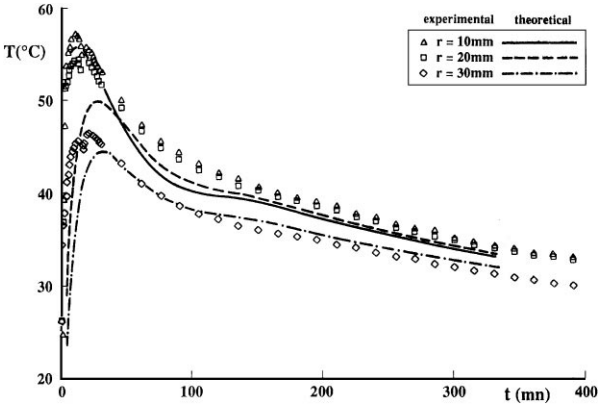

Figure 7. Local temperature evolution during adsorption step. Comparison of model with experimental results. Position of measurements: Δ: $r = a = 10$ mm, $\square$: $r = 20$ mm, $\diamond$: $r = b = 30$ mm.

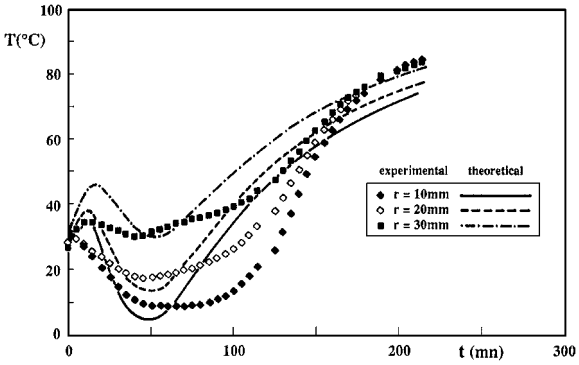

Figure 8. Local temperature evolutions during desorption step. Comparison of model with experimental results. Position of measurements: $\blacklozenge$: $r = a = 10$ mm, $\diamond$: $r = 20$ mm, $\blacksquare$: $r = b = 30$ mm.

course this increase is more important in the outer layers of the cylinder;
— the important temperature decrease that follows is of course the effect of desorption, and is more important near the center of the adsorber, where it is not immediately compensated by the external heating;
— finally, the temperature tends to increase and to become uniform throughout the adsorber, corresponding to the end of desorption and the conventional heating of the adsorber.

The quantitative differences between calculated and measured values are attributed for one part to the fact that the thermal inertia of the metal of the cylinder and the insulation have not been accounted for. However, as observed for the adsorption step, the mass flux parameter, D has probably been underestimated.

Figure 9 compares measured values of the volume of methanol collected in the condenser as a function of time during a desorption step, to calculated values of the amount desorbed (assumed equal to the volume condensed). Again the trends agree, but there is some quantitative deviation. This deviation is consistent with the remarks above: the calculated desorption rate is slower than the measured one during part of the process, and the experimental desorption is terminated earlier. However, the difference in total amount desorbed is unexplained.

(N.B.: the variation of vapour holdup in the system represents a few milliliters, and can therefore account for less than 10% of this difference.)

IV. Discussion

On the Modeling

A question that was open when this work started concerns the degree of sophistication of the model that was necessary to explain the general trends observed. We first developed a "homogeneous" model, that does not account for the radial mass and heat distribution, (but still accounted for the variations of all physical parameters with temperature). With the assumption of local temperature and adsorption equilibria between the fluid and the solid, at constant pressure, the adsorbed quantity becomes a function of temperature T alone, and the model can be put in the form:

$$\frac{dT}{dt} = F(T) \tag{8}$$

which is particularly easy to integrate. This model turned out to predict reasonably well the overall trends in the adsorption step, as illustrated on Fig. 10, (in which the experimental temperature is a volume average of the six local measurements).

However, it fails to account for the complex behaviour observed in desorption, and gives large quantitative deviations (up to 50%) for the amount of methanol cycled, which is a basic measure of the power of the machine as discussed below. For these reasons, no further attention is given to this model. We recall that the purpose of modeling here is to assist in interpreting the observed phenomena, to predict the trends, and to assist in optimization.

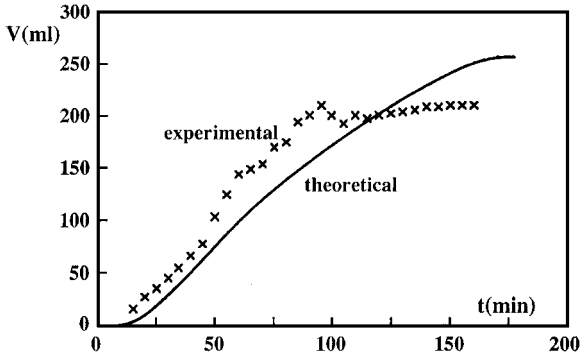

Figure 9. Time evolution of desorbed volume. Comparison of model with experimental result.

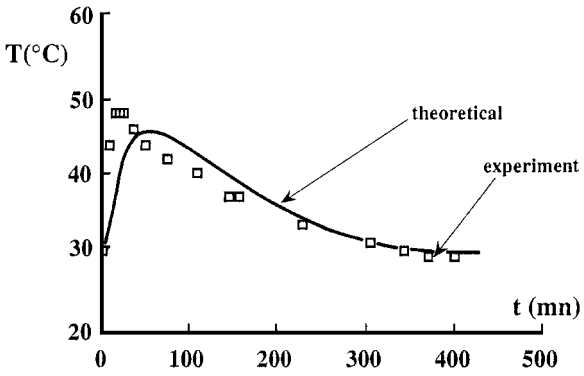

Figure 10. Average temperature evolution during the adsorption step. Comparison of homogeneous model with experimental results.

On the Cooling Capacity

The cooling capacity of the machine is essentially dependent on the amount of methanol evaporated in the evaporator per cycle. One should be aware that a fraction x of the liquid methanol is evaporated in the throttling process, and this process cools the alcohol flow down to the evaporator temperature, but does not contribute to the external cooling power of the machine. The "useful" enthalpy of evaporation per cycle ΔH_e can therefore be expressed as:

$$\Delta H_e = L_v(T_e, P_e) \cdot M_c \cdot (1 - x) \tag{9}$$

where L_v is the mass latent heat of vaporization of methanol at the conditions of the evaporator (T_e, P_e), M_c is the total mass of methanol "cycled", that is evaporated, and then adsorbed and desorbed. Only the fraction $(1 - x)$ of this mixture contributes to the useful cooling effect, and thus to the effective cycled mass. L_v can be considered as a constant for the present purposes: its variation during the experiments, and between experiments, stays within 1%.

The total cycled mass M_c can be expressed as the difference in adsorbed quantity between the conditions of the end of the adsorption step and the condition of the end of the desorption step (T_d, P_d):

$$M_c = [m(T_a, P_e) - m(T_d, P_d)] \tag{10}$$

It can be calculated from the knowledge of the adsorption isotherm (here, using the Dubinin-Radushkevitch approach), and the measured or predicted end conditions (T_a, P_e) and (T_d, P_d). The calculated values of M_c presented here involve the measured values of the pressures, and the values of temperatures calculated by the model. These values are compared to the measured values of the volume of the liquid in the condenser at the end of the desorption step, which is a direct measure of the cycled mass, (this is true after the startup cycle). This is the comparison that is made for example on Fig. 9.

The evaluation of the cooling capacity requires to calculate the vapour fraction x. This is done using an enthalpy balance on the throttling process, assumed isenthalpic, which yields essentially:

$$x = \frac{h_L(T_c, P_c) - h_L(T_e, P_e)}{L_v(T_e, P_e)} \tag{11}$$

The numerator is calculated from the specific heat of methanol as a function of temperature and pressure.

As an example, for $T_e = -10°C$, $P_e = 0.04$ bars and $T_c = 30°C$, $P_c = 0.25$ bars, we find $x = 0.083$, meaning that slightly more than 8% of the methanol is vaporized in the throttling, to cool down the mixture to $-10°C$. In the case corresponding to Fig. 9 (volume of methanol cycled equal to 0.2 liters) the evaporator temperature is $0°C$, and $x = 0.062$, and the cooling capacity is 175 kJ per cycle and per kg of adsorbent.

On the Cooling Temperature

The temperatures reached in the evaporator were measured at the external surface of the evaporator. In the first cycle, the measured temperature was as low as $-10°C$, but for further cycles, it was rather close to $0°C$, and tended to increase slowly. This transient aspect is attributed to the level of vacuum reached in the apparatus, and its evolution. The initial vacuum, with the apparatus completely purged of methanol, is below 1 mbar. When methanol is loaded into the apparatus and evaporated, the pressure typically rises to 10 mbar, at which pressure the boiling temperature would be $-30°C$. The $-10°C$ actually observed are related to the thermal inertia and losses of the evaporator. In subsequent cycles, the "initial" pressure in the evaporator, just when the throttle valve is opened, is determined by the connection with the adsorber, which has been cooled at its lower pressure (lowest point in the diagram of Fig. 5, which corresponds to approximately 10 mbar). The evaporation temperature is then the boiling temperature at the pressure which corresponds to the plateau 1b of Fig. 5 (about 75 mbars) thus a boiling temperature close to $0°C$.

This discussion illustrates how the cooling temperature is related to the pressure levels in the evaporator, but also shows that this pressure level is not easily predictable. It depends on the initial vacuum, before loading the apparatus with methanol, on the amount of methanol loaded, and on the heating and cooling temperatures of the adsorber and of the condenser. A very detailed modeling of the complete apparatus would be required to predict the cooling temperature a priori. This was not done here. In our experiment, due to microleaks, the low pressure point tended to shift slowly, and therefore the cooling temperature showed a slow rise from cycle to cycle.

On the Cooling Power

It does not really make sense to speak of cooling power for such a machine, because the operation is discontinuous, and the time basis for expressing the power is more or less arbitrary. Of course, on a daily basis the power is ridiculously small (2 W!). On the other hand, referred to the first hour (this is approximately the time needed to throttle the total amount of methanol), the power is of the order of 50 W.

On the Methanol Load

Various experiments were run with different methanol loads. An optimal load is found, which maximizes the cycled quantity, and therefore the cooling capacity. This optimal load is found to be 0.3 liters and interestingly, compares closely to the maximal adsorbable volume of the adsorbent ($W_o = 0.37$ cm^3 g^{-1}, thus 0.32 liters for the whole adsorber).

The existence of this optimum is intuitively obvious. When overloaded, the system contains methanol vapours everywhere, it is impossible to obtain low pressures, and a large part of the methanol does not contribute to the useful effect (it actually contributes to the fraction x). When underloaded the system does not make use of the full sorption capacity. The optimum is clearly determined by the full use of the sorption capacity.

V. Conclusion

The results presented here involve experiments made on a prototype of adsorption refrigerator, in which the time evolution of temperatures, pressures and cumulated flows have been measured at various places in the apparatus. In particular, temperatures have been measured radially inside the annular activated carbon layer constituting the adsorber.

As the adsorption necessarily works in cycles, multiple transient phenomena occur, at different time scales. Short time transients are produced by pressure changes due to valve opening or closing. Somewhat longer transients are due to the heat and mass transfer dynamics of the adsorber during one particular step of the cycle; the succession of steps of course determines the overall period of the cycle, but also, the behaviour of the system evolves from cycle to cycle from the start-up, until a truly periodic regime is reached. In this study, we have tried to approach this periodic regime. In most cases, the start-up is distinctly different because the activated carbon is initially perfectly clean (it has been regenerated by vacuum heating for several days), but the second-cycle is already quite close to the periodic regime. This is particularly true because our cycles were relatively long (several hours) so that most of the important cycle transients occur at the beginning. This may no longer be true for shorter cycles, and the complete transient model developed may prove useful in evaluating these effects. The superposition and the coupling between the various transient phenomena produce an apparently complex overall behaviour, which is nevertheless explainable and relatively predictable.

We have shown that a lumped model, not accounting for the detailed profiles in the adsorbent, will not give correct predictions of the transient evolutions. On the other hand a relatively simple model accounting for these profiles distinctly improves the predictions if one neglects the very short pressure transients. Let us emphasize that in the model used, no parameter was adjusted, but some key parameters, such as the thermophysical properties, were obtained from correlations of the literature. Note also that the heat inertia of the apparatus and the insulation, neglected here but certainly influent, would probably be less important in a full size apparatus.

Appendix: Thermophysical Data

Methanol, Ethanol

The specific heats of the vapour and the liquid, the liquid thermal conductivity and the vapour pressure were obtained in the range (-50; $+130^\circ$C) from Raznjevic (1970).

Activated Carbon (AC35/3 of CECA, France)

The total porosity, the specific heat and the thermal conductivity are taken from Onyebueke (1989).

Total porosity: 0.72

Specific heat: $C_{vs} = 1020$ J kg^{-1} K^{-1} at 30°C

$C_{vs} = 1250$ J kg^{-1} K^{-1} at 100°C

Expression of thermal conductivity λ, in W m^{-1} K^{-1}:

— in vacuum:

$$\lambda_{\text{eff}} = 0.0318 + 1.872 \times 10^{-4}\, T + 7.407 \times 10^{-7} T^2$$

— as a function of alcohol vapour pressure:

Methanol

$$27^\circ\text{C} \quad \lambda = 0.0972 + 0.008\,\text{Ln}P + 7.122 \times 10^{-4}\,\text{Ln}^2 P - 7.49 \times 10^{-5}\,\text{Ln}^3 P - 5.822 \times 10^{-6}\,\text{Ln}^4 P$$

$$60^\circ\text{C} \quad \lambda = 0.1156 + 0.0089\,\text{Ln}P - 1.257 \times 10^{-4}\,\text{Ln}^2 P - 1.013 \times 10^{-4}\,\text{Ln}^3 P + 5.671 \times 10^{-6}\,\text{Ln}^4 P$$

Ethanol

$$27^\circ\text{C} \quad \lambda = 0.0963 + 0.0077\,\text{Ln}P + 7.685 \times 10^{-4}\,\text{Ln}^2 P - 6.879 \times 10^{-5}\,\text{Ln}^3 P - 8.338 \times 10^{-6}\,\text{Ln}^4 P$$

$$60^\circ\text{C} \quad \lambda = 0.114 + 0.0087\,\text{Ln}P + 1.408 \times 10^{-5}\,\text{Ln}^2 P - 1.042 \times 10^{-4}\,\text{Ln}^3 P + 3.975 \times 10^{-6}\,\text{Ln}^4 P$$

Energy of Adsorption

Δu_{ad} is calculated by combining the Gibbs-Helmholtz equation with the Dubinin-Raduschkevith isotherm.

$$\Delta u_{\text{ad}} = RT + L_{\text{v}} + \Delta G_{\text{diff}} - T\,\Delta S_{\text{diff}}$$

where L_{v} is the latent heat of vaporization, and ΔG_{diff} and ΔS_{diff} are given by

$$\Delta G_{\text{diff}} = \varepsilon' = RT \ln \frac{P_0}{P}$$

$$\Delta S_{\text{diff}} = \alpha \left(\frac{\partial \varepsilon'}{\partial \ln C} \right)_T$$

By introducing the D.R. isotherm (Eq. (6)), as shown by Boussehain (1986) we obtain:

$$\Delta u_{\text{ad}} = RT + L + \frac{2{,}303\beta}{\sqrt{k}} \times \left[\ln^{1/2}\left[\frac{1}{\theta}\right] + \frac{\alpha T}{2} \ln^{-1/2}\left[\frac{1}{\theta}\right] \right]$$

where α is the thermal expansion coefficient of the liquid, and $\theta = \frac{q}{q_{\text{m}}}$.

Diffusivity

The diffusivity or pure vapour permeability introduced in Eq. (1) is a fluid phase diffusivity, corrected empirically to account for the bidisperse porosity, as proposed by Furusawa (1973). Finally, the relation used has the form

$$D = AD_0 \exp(\theta B(T))$$

where D_0 is the vapour phase self diffusivity of alcohol, θ is the coverage, and A and B are parameters given in Luo (1991). Thus D is recalculated for each adsorbed concentration and temperature.

Nomenclature

a	Inner radius of annulus (m)
b	Outer radius of annulus (m)
C_{vg}, C_{va}	Specific heats of gas and adsorbate respectively ($\text{J mol}^{-1}\,\text{K}^{-1}$)
C_{vs}	Specific heat of clean adsorbent ($\text{J kg}^{-1}\,\text{K}^{-1}$)
C	Molar concentration of gas (mol m^{-3})
C_{f}	Concentration of the vapour from the evaporator (mol m^{-3})
D	Effective diffusivity introduced in Eq. (1) and Appendix ($\text{m}^2\,\text{s}^{-1}$)
k	Coefficient in Dubinin-Raduschkevitch equation (Eq. (6)) (-)
K_{o}	Heat transfer coefficient from wall of adsorber to outside ($\text{W m}^{-2}\,\text{K}^{-1}$)
K_{i}	Heat transfer coefficient from bulk gas to adsorbent ($\text{W m}^{-2}\,\text{K}^{-1}$)
L	Length of the adsorber (m)
L_{v}	Latent heat of vaporization of alcohol (J mol^{-1})
m_{tot}	Total amount of alcohol processed (kg)
$m_{\text{e}}\, m_0$	Molar flow rates at bed entrance and at bed outlet respectively (mol s^{-1})
P	Pressure (Pa)
P_{sat}	Saturation pressure (Pa)
P_{u}	External heating power (W)
q	Adsorbed concentration (mol kg^1 absorbent)
q_{m}	Maximum adsorbed concentration (mol kg^{-1} adsorbent)
Q_{tot}	Total adsorbed quantity (mol)
r	Radius of the adsorber (m)

R	Constant of perfect gas
T_a	Equilibrium adsorption temperature (K)
T_{ia}	Initial adsorption temperature (K)
T_{id}	Initial desorption temperature (K)
T_g, T_e	Gas temperature inside adsorber and at adsorber inlet respectively (K)
T_s	Solid temperature in adsorber (K)
T_o	Ambient temperature (K)
Δu_{ad}	Energy of adsorption ($J\,mol^{-1}$)

Greek Letters

β	Coefficient in Dubinin-Raduschkevitch equation (Eq. (6)) ($J\,mol^{-1}$)
ε	Total porosity, volume fraction occupied by gas (-)
ε'	Polanyi adsorption potential (Eq. (6) and (7)) ($J\,mol^{-1}$)
λ_{eff}	Effective conductivity of the adsorbent ($J\,m^{-1}\,K^{-1}$)
ρ_s	True density of solid adsorbent ($kg\,m^{-3}$)

Subscripts

a	Adsorbed phase
g	Gas phase
e	Entrance, inlet
i	Initial
o	Outlet
s	Solid phase

Superscript

•	Indicates a time derivative

Acknowledgment

The experimental results used here were obtained at the Laboratoire d'Energétique et de Mécanique Théorique et Appliquée (ENSEM-INPL Nancy, France), in the framework of the doctoral thesis of L. LUO. These results are presented more extensively in a seperate article (Luo and Feidt, 1997).

References

1. Boussehain, R., "Caractérisation thermostatique et cinétique des phénomènes d'adsorption-désorption de couples charbons actifs-alcools," Thesis I.N.P.L., Nancy, France, 1986.
2. Critoph, R.C. and R. Vogel, "Possible Adsorption Pairs for Use in Solar Cooling," *International Journal of Ambient Energy*, **7**(4), 183–190 (1986).
3. Furusawa, T. and J.M. Smith, "Diffusivities from Dynamic Adsorption Data," *AIChE J.*, **19**(2), 401–403 (1973).
4. Lu, H.B., N. Mazet, and B. Spinner, "Modelling of Gas-Solid Reactions—Coupling of Heat and Mass Transfer with Chemical Reaction," *Chem. Engng. Science*, **51**, 3829–3845 (1996).
5. Luo L., "Etude thermodynamique et thermique de machine à adsorption à cycle inverse à adsorption," Thesis INPL, Nancy, France, 1991.
6. Luo, L. and M. Feidt, "Comportement transitoire d'une machine frigorifique à adsorption. Etude expérimentale du système alcool/charbon actif," *Rev. Gle. Thermique*, **36**, 159–169 (1997).
7. Luo, L., M. Feidt, and R. Boussehain, "Etude thermodynamique de machine à cycle inverse à adsorption," *Entropie*, **183**, 3–11 (1994).
8. Onyebueke, L.C., "Etude des transferts de chaleur au générateur de machines trithermes à adsorption," Thesis I.N.P.L., Nancy, France, 1989.
9. Raznjevic, K., "Tables et diagrammes thermodynamiques," Edition Eyrolles, Paris, 1970.
10. Ruthven, D.M., *Principles of Adsorption and Adsorption Processes*, John Wiley, New-York, 1984.
11. Sakoda, A. and M. Suzuki, "Fundamental Study on Solar Powered Adsorption Cooling Systems," *J. Chem. Engng. Japan*, **17**(1), 52–57 (1984).
12. Sun, L.M. and F. Meunier, "Non-Isothermal Adsorption in a Bidisperse Adsorption Pellet," *Chem. Engng. Science*, **42**(12), 2899–2907 (1987).
13. Suzuki, M., *Adsorption Engineering*, Kodansha/Elsevier, Tokyo/Amsterdam, 1990.
14. Yang, R.T., *Gas Separation by Adsorption Processes*, Butterworths, Boston, 1987.